Electrical Power and Energy Systems 135 (2022) 107468

Contents lists available at ScienceDirect

International Journal of Electrical Power and Energy Systems

journal homepage: www.elsevier.com/locate/ijepes

A convolutional neural network-based approach to composite power system reliability evaluation

Md. Kamruzzaman *, Narayan Bhusal, Mohammed Benidris

Department of Electrical and Biomedical Engineering, University of Nevada, Reno, NV 89557–0260, USA

ARTICLE INFO

Keywords:
Composite systems
Machine learning
Monte-Carlo
Neural network
Reliability indices

ABSTRACT

This paper proposes a machine learning-based approach in conjunction with Monte Carlo simulation (MCS) to improve the computation efficiency of composite power system reliability evaluation. Traditional composite system reliability evaluation approaches are computationally demanding and may become inapplicable to large integrated power grids due to the requirements of repetitively solving optimal power flow (OPF) for a large number of system states. Machine learning-based approaches have been used to avoid solving OPF in composite system reliability evaluation except in the training stage. However, current approaches have been derived to classify system states into success and failure states (i.e., up or down). In other words, they can be used to evaluate power system probability and frequency reliability indices, but they cannot be used to evaluate power and energy reliability indices unless OPF is solved for each failure state to determine minimum load curtailments. In this paper, a convolutional neural network (CNN)-based regression approach is proposed to determine the minimum amount of load curtailments of sampled states without solving OPF, except in the training stage. Minimum load curtailments are then used to evaluate power and energy indices (e.g., expected demand not supplied) as well as to evaluate the probability and frequency indices. The proposed approach is applied on several systems including the IEEE Reliability Test Systems (The IEEE RTS and IEEE RTS-96) and Saskatchewan Power Corporation in Canada. Results show that the proposed approach is computationally efficient (fast and accurate) in calculating the most common composite system reliability indices. The developed source code of the proposed method is available to the community for future research and development.

1. Introduction

With the increasing dimensionality and uncertainties of modern power grids, practical application of traditional composite system reliability evaluation methods has become a bottleneck due to their heavy computational burden. Machine learning (ML) algorithms can be a promising solution to reduce certain computational complexities—requirement of solving optimal power flow (OPF)—in the composite system reliability evaluation. Existing ML-based reliability evaluation methods [1–6] use classification algorithms, which are abortive in calculating energy and frequency indices of composite systems. Therefore, it has become indispensable to develop computationally efficient reliability evaluation methods that can calculate not only probability indices but also energy and frequency indices of composite systems. Regression-based ML algorithms have the potential to efficiently evaluate probability, energy, and frequency indices of composite systems, which are developed, discussed, and demonstrated in this paper.

Several methods have been proposed in the literature to reduce the computation burden and convergence time of composite system reliability evaluation [7–23]. Among these methods, population-based intelligent search (PIS) methods have been used in [7–18] to reduce the computation burden of power system reliability evaluation. These search-based reliability evaluation methods generally have two steps. In the first step, PIS methods, such as genetic algorithm [7], the modified genetic algorithm [8], the state space pruning [9–15], and particle swarm optimization [16–18], are used to reduce the size of state space. In the second step, Monte Carlo simulations (MCSs) are performed on the reduced state space to compute reliability indices. In [19], the required number of samples to evaluate the reliability of composite systems has been reduced using non-sequential MCS with a cross-entropy-based optimization method. A multi-parametric linear programming-based approach has been proposed to decrease the requirement of solving OPF in composite power system reliability

* Corresponding author.
E-mail addresses: mkamruzzaman@nevada.unr.edu (Md. Kamruzzaman), bhusalnarayan62@nevada.unr.edu (N. Bhusal), mbenidris@unr.edu (M. Benidris).

https://doi.org/10.1016/j.ijepes.2021.107468
Received 11 December 2020; Received in revised form 14 June 2021; Accepted 28 July 2021
Available online 13 August 2021

evaluation [20]. In [21], a hierarchical decoupling optimization framework and impact-increment-based state enumeration method has been proposed to increase the accuracy and calculation speed of power system reliability evaluation with integrated energy systems. An improved estimation of distribution algorithm-based approach has been proposed in [22] to increase the speed of composite power system reliability evaluation using MCS by reducing the requirements of repeatedly solving OPF. In [23], an intelligent state space reduction and pseudo-sequential MCS-based approach has been proposed to reduce the computational burden of composite systems reliability evaluation with photovoltaic energy sources. Although the proposed methods in [7–23] reduce the number of sampled states that require solving OPF for reliability evaluation, they still require to perform the OPF for a significantly large number of system states.

Several ML-based methods have been proposed in the literature to reduce/avoid the requirement of performing the OPF for composite system reliability evaluation [1–6,24–28]. A least-squares support vector machine classifier-based reliability evaluation method has been proposed in [1], which requires performing the OPF in both training stage and evaluation stage (i.e., perform OPF on classified failure states by the trained network to calculate reliability indices). A multi-label k-nearest neighbor classification algorithm-based method has been proposed in [2], which utilizes the OPF for the training samples to calculate the Loss of Load Probability (LOLP) index. In [3], a method based on a multi-label radial basis classification technique, importance sampling, and MCS has been proposed to calculate the LOLP using the OPF for training samples. In [4,5], the authors have combined the group method data handling-based classification algorithm with non-sequential MCS to evaluate the reliability of composite systems. However, the calculated indices in [4,5] are imprecise as compared with the benchmarked results provided in [1,29,30] for the adapted systems. A self-organizing map-based classification algorithm with MCS has been used in [6] to calculate the LOLP index. A Bayesian network-based classification approach has been proposed in [24] to calculate the loss of load (LOL) index. In [25], a selection approach has been proposed to select training samples and training convolutional neural networks to calculate the LOLP of power systems. In [26], a Long Short Term Memory (LSTM)-based neural network has been used to calculate the LOLP in adequacy-based power system reliability assessment considering renewable resources. Another LSTM-based approach has been proposed in [27] to calculate the LOLP of composite power systems with wind farms. An artificial neural network-based method to model the output from wind and solar generators in power system reliability evaluation has been proposed in [28].

The methods proposed in [1–6,24–28] solve OPF in the training stage to classify system states in the evaluation stage into either success or failure states without determining the amount of load curtailments, which is sufficient only for determining the LOLP and Loss of Load Frequency (LOLF) indices. However, OPF has to be solved for each sampled failure state to determine the amount of load curtailment, which is needed to determine the Expected Demand Not Supplied (EDNS) index. The EDNS index provides a measure to the severity of failure states. Thus, the classification-based methods proposed in [1–6,24–28] are effective in calculating the LOLP and LOLF indices, but cannot be directly applied to calculate the EDNS index. Therefore, it is critical to develop a method to determine amounts of load curtailments during failure states without solving OPF for each sampled state in the evaluation stage.

In this paper, a convolutional neural network (CNN)-based approach is proposed to calculate the well-known composite system reliability indices (i.e., LOLP, LOLF, and EDNS) without performing OPF, except in the training stage. The proposed approach starts with training the CNN using historical data. Then, the trained CNN is used to predict load curtailments for each sampled system state, which are used to calculate the reliability indices. In the next step, sampled system states are classified into failure and success states based on predicted load curtailments. In the last step, predicted load curtailments are directly used to calculate the EDNS while classified system states are used to calculate the LOLP and LOLF indices. The LOLF is calculated using the classified system states and failure and repair rates of system components. Main contributions of the proposed work in comparison with existing methods are summarized as follows.

- Development of an effective CNN-based approach to calculate the well-known reliability (probability, energy, and frequency) indices of power systems without performing OPF except in the training stage, which reduces the computational burden and time significantly compared to the existing methods. The CNN-based approach can accurately incorporate graph structures of power systems (grid-like topology), which provides the flexibility of determining minimum load curtailments without performing OPF in the proposed method.
- The proposed CNN-based approach improves the scalability issues of existing ML-based methods in calculating energy indices by eliminating the requirement of solving the OPF for failure states.
- A data generation scheme is developed based on the availability of system components, hourly loads, and network constraints to generate diverse historical data for both training the CNN and calculating the reliability indices.

The proposed method is applied on IEEE Reliability Test System (The IEEE RTS and IEEE RTS-96) and Saskatchewan Power Corporation in Canada (SPC) to demonstrate its effectiveness on various system sizes and typologies.

The rest of the paper is arranged as follows. Section 2 describes the data generation scheme for the proposed composite system reliability evaluation method. Section 3 provides procedures to calculate the composite system reliability indices using the proposed method. Numerical examples to demonstrate the effectiveness of the proposed method are presented in Section 4. Section 5 provides some concluding remarks.

2. Data generation scheme

In the training phase, a set of system states is randomly generated and OPF is solved for each state—the OPF is solved only in the training stage. Available generation and statuses of transmission lines are provided as input and load curtailments (i.e., no load curtailments for up states) at respective states are used as the output to train a CNN. The trained CNN is used with MCS in the evaluation phase to determine minimum load curtailments of sampled states and evaluate composite system reliability indices. The main advantage of this approach is to use CNN to eliminate the need for solving OPF for each sampled state and that to determine minimum load curtailments for failure states.

2.1. Input and output parameters for training

Composite system reliability evaluation depends on network topology, bus load conditions, and availability of generators and transmission lines. Generators and transmission lines may not be available due to several reasons including scheduled maintenance and forced outages. In the proposed method, system states are sampled based on the availability of generators and transmission lines and total loads of system buses (bus loads are considered variable loads when calculating annual indices and considered fixed at the peak load when calculating annualized indices). In each sampled state, each component can be in either up (available) or down (unavailable) state based on its mean time to failure and mean time to repair rates. A binary string is used to represent the operating state of a component (i.e., ‘1’ represents down/failure state or malfunctioning and ‘0’ represents up/normal state and functioning). In this work, we generate random numbers and compare them with the availability of system components to sample system states. The

operating state of each component of a sampled system state is expressed as follows.

$$S = \begin{cases} 1, & \text{if } r_p \leqslant \mathcal{A}_p, \quad p = 1, 2, \cdots, P \\ 0, & \text{otherwise} \end{cases} \tag{1}$$

where P is the total number of system components; r_p is the generated random number for p^{th} component; $\mathcal{A}_p$ is the availability of the p^{th} component; and S is a $P \times 1$ vector that represents operating states of all the system components.

The efficiency of a trained neural network depends on the selection of input variables with well-defined corresponding output (target) patterns in the training data set. In the proposed reliability evaluation method, the available power generation at each bus, capacities of transmission lines, and loads are used as input parameters and load curtailments are used as the target to train the CNN. An input vector for the proposed approach is expressed as follows.

$$I = \left[G_1, G_2, \cdots, G_M, C_1, C_2, \cdots, C_{N_t}, \left(\sum_{i=1}^{N_\ell} L_i \right) \right], \tag{2}$$

where M is the total number of buses that have generators; N_ℓ is the number of load buses; N_t is the total number of transmission lines; G_M is the sum of available generation at bus M; C_{N_t} is the capacity of transmission line N_t; L_i is the load demand of bus i; and I is the input training vector.

It is worth mentioning here that the capacity of a failed line in (2) is set to zero only as an input parameter to train the machine learning in case of failure of the line, which helps to capture the nonlinear relationship between the input and output data of the machine learning model. When calculating the load curtailment using OPF, the failed lines are considered open circuits. Also, a constant power load model is used in power flow (steady-state) analysis to generate training samples, which is widely used in composite system reliability evaluation.

Outputs from renewable generators can be calculated using existing models for renewable energy sources. In this work, we have used the proposed artificial neural network-based approach in [28] to calculate outputs from wind and solar generators in power system reliability evaluation methods. As the main objective of the proposed work is to reduce the computational burden of reliability evaluation methods, instead of reproducing rigorous models presented in [28], we provide main steps of modeling output power from wind and solar generators, which are: (i) collecting data for hourly mean wind speed and solar irradiances, hourly standard deviations, wind energy, and solar energy data for the entire year, (ii) developing a multi-state model using artificial neural network, (iii) calculating wind speed and solar irradiance data transitions rates using discrete Markov chains, (iv) modeling of wind turbine output power based on cut-in-and cut-out speed, and (v) modeling of solar panel output power based on beta probability density function.

The targets (load curtailments) to train the CNN is expressed as follows.

$$T = \left[\left(\sum_{i=1}^{N_\ell} L_i^c \right) \right], \tag{3}$$

where L_i^c is the minimum amount of load curtailment at bus i and T is the corresponding output (target).

2.2. Network modeling

The linearized power flow model (DC power flow model), which has been widely used in composite system reliability evaluation, is utilized in this paper to determine minimum load curtailment to train the CNN. The objective function to minimize load curtailments for training samples can be expressed as follows [31].

$$\text{Minimize} \quad (\textit{Load curtailment}) = \min \left(\sum_{i=1}^{N_\ell} L_i^c \right) \tag{4}$$

The network constraints subject to the objective function (4) are as follows.

Power balance equations,

$$B\theta + G + L^c = L \tag{5}$$

where B is an $(N \times N)$ matrix that represents bus susceptance; θ is an $(N \times 1)$ vector of nodal voltage angles; G is an $(N \times 1)$ vector of power generation at buses; L^c is an $(N \times 1)$ vector of load curtailments; L is an $(N \times 1)$ vector of load demand; and N is number of system buses.

Real power generation constraints,

$$G_i^{min} \leqslant G_i \leqslant G_i^{max} \tag{6}$$

where G_i^{min} and G_i^{max} are respectively the minimum and maximum power generation limits at bus i.

Line capacity constraints,

$$-F^{max} \leqslant B_l A\theta \leqslant F^{max} \tag{7}$$

where F^{max} is the vector of maximum capacities of transmission lines $(N_t \times 1)$; B_l is a diagonal $(N_t \times N_t)$ matrix where its diagonal elements are transmission line susceptances; and A is the element-node incidence matrix $(N_t \times N)$.

Load curtailment constraints,

$$0 \leqslant L^c \leqslant L \tag{8}$$

Node voltage angle constraints,

$$-\pi \leqslant \theta \leqslant \pi \tag{9}$$

In order to achieve a feasible solution, one of the bus angles has been assumed as zero for the given constraints in (5)–(9).

3. The proposed approach for composite power system reliability evaluation

This section describes the architecture of convolutional neural network used in this work, training attributes of the proposed approach, and the proposed mechanism to determine composite power system reliability indices.

3.1. Convolutional neural network

Convolutional Neural Networks (CNNs) have been used in several applications. Variant of CNN model applied in [32] for image classification won the ILSVRC-2012 competition after which CNN received significant attention from researchers all around the world. We used CNN because it has the capability to accurately incorporate graph structures of power systems (grid-like topology), which is similar to image structure in image classification tasks. It has been successively applied in various power system related prediction and classification problems [33–41]. In power system, CNN has been used with 1-dimensional (1-D) input dataset as well as multi-dimensional dataset. Some of the examples that use 1-D input for power system problems similar to proposed work are as follows. CNN and LightGBM are combined in [34] for ultra-short-term wind power forecasting in which 1-Dimension (1-D) (containing various features including wind speed, temperature, etc.) vector is used as an input to the proposed model. In [35], photovoltaic power has been forecasted using deep CNN with 1-D input vector for the CNN model. Location of false data injection attack has been detected in [36] using CNN through multi-label classification approach in which the input of the CNN architecture is the 1-D measurement vector. In [41],

recurrent inception CNN is used for multi short-term load forecasting which also uses various 1-D features for input for the CNN architecture. Due to its ability to capture complex patterns within power system measurements and states, CNN is used in this work to replace OPF in determining minimum load curtailments. Other benefits of CNN is that it is easier to train, can automatically extract system features, and have fewer parameters compared to the fully connected neural network with the same number of hidden units. CNNs generally have a convolutional layer followed by a pooling layer. The convolutional and pooling layers find the low level feature of the input vector. Fully connected layers are added after the convolutional and pooling layers to predict the output. Although CNN architecture is well-suited for 2-D input, it can be used efficiently for 1-D inputs like the proposed work. In the proposed work, the pooling layer doesn't have any significant impact; therefore, only convolutional and dense layers are used. Fig. 1 shows the architecture of CNN for the proposed work. The feature map of the CNN and the dense layers is described as follows.

The feature map generated by the input layer can be expressed as follows.

$$cnn_1 = \sigma(z_t * h_1 + b_1) \tag{10}$$

where h_1 is a convolutional kernel (1-D filter) and b_1 is bias vector. Similarly, the feature map of the hidden layer can be presented as follows.

$$cnn_q = \sigma(cnn_{q-1} * h_q + b_q) \tag{11}$$

where cnn_{q-1} is the feature map of the $(q-1)$-th layer, and h_q and b_q are convolutional kernel and bias vector of the q-th layer, respectively. Before outputting the final results from the final dense layer, a fully connected layer is required to flatten the last convolutional layer. The feature map of the hidden fully connected (FC) (dense) layer can be expressed as follows.

$$flat_{cnn} = \sigma(w_f * cnn_{last} + b_f) \tag{12}$$

where cnn_{last} is the feature map of the last layer of the hidden convolutional layers, and w_f and b_f are respectively the weight and bias vectors of the hidden dense layer. The feature map of the final output dense layer is as follows.

$$\widehat{T} = \sigma(w_d \times mlp_{d-1} + b_d) \tag{13}$$

where w_d and b_d are the weight and bias of the output layer and mlp_{d-1} is the feature map of the layer just before the final layer.

3.2. Training attributes

To use the proposed model, we need to train it to optimize the learning parameters such as weights, w, and bias, b, in each layer. The optimized parameters can map the relationship between the input vector and the output load curtailments.

Following the normal trend in the machine learning, the training and testing dataset are separated as 7/10 and 3/10. Mini-batch size of 64 and number of epochs of 200 are used. We have adopted the commonly used mean absolute error (MAE) as loss function which is the arithmetic average of absolute error between predicted load curtailment and the actual load curtailment. Adaptive moment estimation (Adam) is adopted as an optimizer to obtain the optimal parameters.

3.3. Selection of training samples

Typically, the failure probability of power systems is very low. Therefore, the probability of success subspaces of a power system is much larger than the probability of failure subspaces. If all the sampled states of a power system are taken into consideration for training the neural networks, then a very large number of samples is required in the training data set. This will eventually demolish the goal of reducing the computational cost of power system reliability evaluation using machine learning algorithms. In [2], most of the success states are discarded to generate a balanced training data set with reduced size. In [1,4], two success states for each failure state are selected to generate a more balanced training data set. It is worth mentioning here that a large number of repeated patterns of the input and output vectors remain in the power system states due to the high availability of system components, which may cause overtraining for the used training samples in [2,1,4]. Therefore, in this work, repeated states are removed from the training data set to train the algorithm on a diverse set of states. In calculating the annual indices, load levels are also added to the criterion of removing repeated states. Then, the OPF is performed to determine targets for the generated data set. It should be noted that the size of the data set needs to be large enough to contain a reasonable number of success and failure states, which can be determined by analyzing the training performance of the CNN. Also, it is worth mentioning here that power systems are typically very reliable and most of the samples will have no load curtailment for annual reliability evaluation. In this work, following the same convention of [3,42], we have used load clusters to calculate annual reliability indices, and the CNN is trained only for the load clusters that have load curtailments. The annual reliability indices of the system are calculated based on the weight of each cluster.

3.4. The proposed method to Compute Reliability Evaluation

After training the CNN, system states (total available generation and loads) are sampled based on the procedure described in Section 2.1. Then, sampled system states are fed as input to the trained CNN and predicted load curtailments are used to calculate the reliability indices

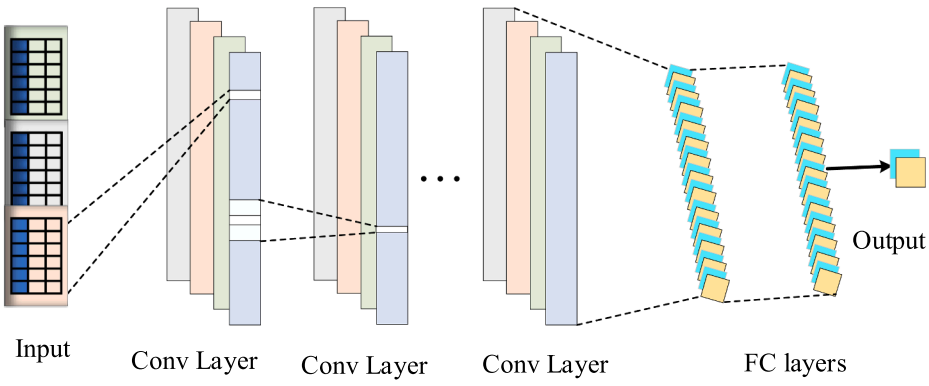

Fig. 1. Architecture of 1-Dimensional CNN for the proposed work. The Input in the figure are generations injected at generation buses, line capacities of all the lines, and the total loads of the system. The output is the total load curtailments of the system for the given input parameters.

including the LOLP, EDNS, and LOLF indices. The definitions and procedure to calculate the reliability indices are presented as follows.

3.4.1. Calculation of EDNS

The EDNS index is used to measure the expected amount of load shedding due to system failure to meet the demand. In this work, predicted load curtailments by the trained CNN are directly used to calculate the EDNS index. The expression to calculate the EDNS is as follows.

$$EDNS = \left(\frac{1}{N_s}\sum_{s=1}^{N_s} y_s\right), \tag{14}$$

where N_s is the total number of samples from MCS; and y_s is the predicted load curtailment by the trained CNN for the s^{th} input sample.

3.4.2. Calculation of LOLP

The LOLP index is used to measure the probability of system failure. Thus, instead of using the predicted load curtailments, system states are classified into failure and success states to calculate the LOLP. The predicted outputs from the proposed model are used to classify the system states. A system state is represented by a binary string—'1' represents failure state and '0' represents success state. The expression to calculate the LOLP is as follows.

$$LOLP = \left(\frac{1}{N_s}\sum_{s=1}^{N_s} L_k\right), \quad L_k = \begin{cases} 0, & \text{if } y_s = 0 \\ 1, & \text{if } y_s > 0 \end{cases} \tag{15}$$

3.4.3. Calculation of LOLF

The LOLF index represents the measure of how often a power system fails. It is worth mentioning here that the calculation of LOLF using the system states is not a straight forward process. However, the proposed method in [10] can be adopted to determine the LOLF. Instead of reproducing the rigorous procedure provided in [10], we provide only the required expressions to calculate the LOLF based on our proposed method, which are as follows.

$$LOLF = \left(\frac{1}{N_s}\sum_{s=1}^{N_s} \phi_s\right), \tag{16}$$

where,

$$\phi_s = \begin{cases} \sum_{i=1}^{N}(\lambda_i^+ - \lambda_i^-), & \text{if } y_s > 0 \\ 0, & \text{if } y_s = 0 \end{cases} \tag{17}$$

where λ_i^+ is the transition rate of component i from its state in failure state to higher states; and λ_i^- is the transition rate of component i from its state in failure state to lower states.

3.4.4. Convergence criterion to calculate the indices

A convergence criterion needs to be applied to stop the algorithm when the reliability indices reach a steady state. The coefficient of variance of reliability indices is usually used as a convergence criterion in power system reliability studies, which is adapted in this work. The coefficient of variance of a reliability index is expressed as follows [43].

$$\beta = \frac{\sqrt{Var(RI)}}{E(RI)}, \tag{18}$$

where β is the coefficient of variance of a reliability index; and RI is the reliability index. The proposed algorithm is performed until the value of β reaches a predefined tolerance level, ϵ.

In reliability evaluation studies of power systems, the energy indices have been observed as the slowest indices in terms of convergence using MCS [44]. Following the same convention, we applied the stopping criterion on the EDNS index in this work. A flowchart to evaluate the composite system reliability using the proposed method is shwon in Fig. 2.

3.5. Performance evaluation metrics

Evaluation metrics used to evaluate the performance of the machine learning model are as follows. Mean absolute error (MAE) and root mean square error (RMSE) are used to evaluate the prediction (regression) performance of the model (predicted load curtailment is used to calculate EDNS). The classification dataset to calculate LOLP and LOLF are determined using a threshold (different value of threshold are used based on their load levels) in the predicted load curtailment. That is, if the predicted curtailment is more than the threshold, label '1' (down/failure state) is used, and if the curtailment is below the threshold label '0' (normal/up state) is used. The predicted labels are compared with the actual labels and the classification performance is evaluated using precision, recall, and the F_1-score.

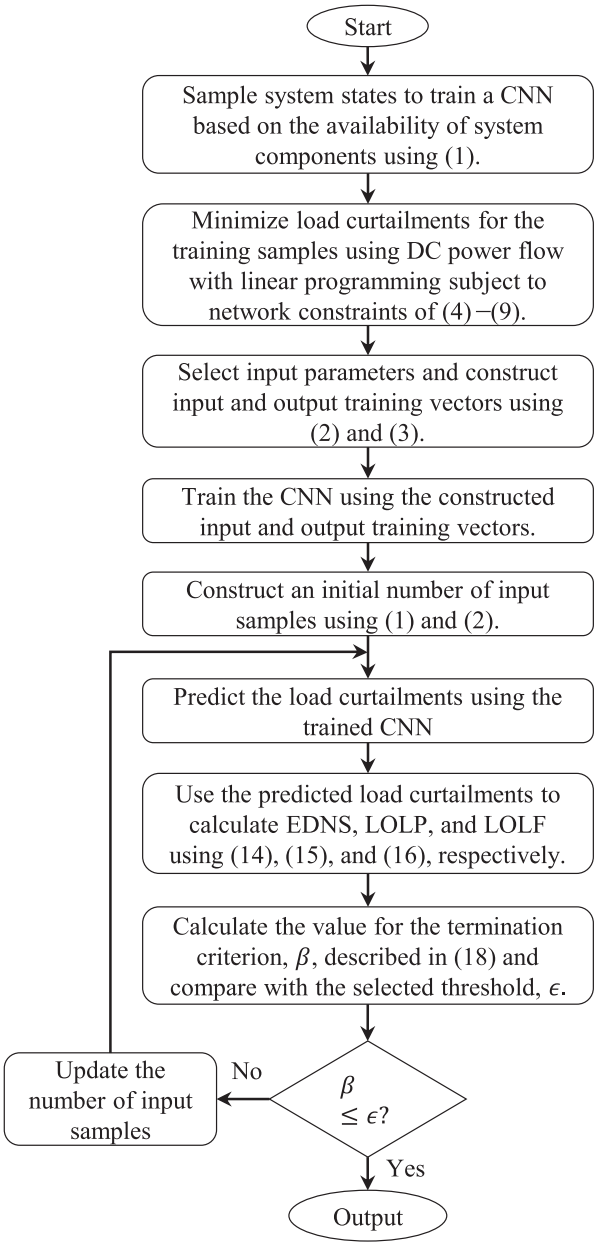

Fig. 2. Flowchart to calculate reliability indices for composite power systems using the proposed method.

1. Mean Absolute Error (MAE):

$$MAE = \frac{1}{N}\sum_{t=1}^{N}|x^t - \hat{x}^t| \tag{19}$$

2. Root Mean Square Error (RMSE):

$$RMSE = \sqrt{\frac{1}{N}\sum_{t=1}^{N}\left(x_i^t - \hat{x}_i^t\right)^2} \tag{20}$$

3. Precision: It is the fraction of true predicted positive labels among all positive predicted labels, which can be expressed as follows.

$$P = \frac{T_p}{T_p + F_p} \tag{21}$$

4. Recall: It is the fraction of true predicted positive labels among the actual positive labels, which can be expressed as follows.

$$R = \frac{T_p}{T_p + F_n} \tag{22}$$

5. F_1-Score: It is the harmonic mean of precision and recall, which can be expressed as follows.

$$F_1 - \text{Score} = 2 \times \frac{P \times R}{P + R} \tag{23}$$

where N is the total number of test samples; and x^t and $\hat{x}^t$ represent actual and predicted states, respectively. T_p represents true positive—down states labeled as down states; T_n denotes true negative—up states labeled as up states; F_p denotes the false positive—up states labeled as down states; and F_n is false negative—down states labeled as up states.

4. Numerical examples

The proposed method is demonstrated on the IEEE RTS [45], SPC in Canada [46], IEEE RTS-96 [47]. It is worth mentioning here that these systems are selected due to the variations in their sizes, line constraints, loading levels, and availability of system components. For example, the SPC system has more capacity margin than IEEE RTS and IEEE RTS-96, which makes it less stressful than the IEEE RTS and IEEE RTS-96. Also, several load curtailment scenarios are found during annualized reliability evaluation of the SPC system with the mean load while the IEEE RTS and IEEE RTS-96 has no curtailments for the mean load. Moreover, the probability of all the system components are being in the up states for the SPC is 0.44306 and that for the IEEE RTS and IEEE RTS-96 are 0.23044 and 0.01218, respectively. The training and testing dataset required for each of the systems is generated using the procedure described in Section 2. The reliability indices are calculated using the proposed method.

Also, reliability indices for the adapted systems are calculated using the MCS, which are used as references to analyze the accuracy of the proposed method. To evaluate the reliability indices using the MCS, the system states are sampled using (1) and (2). Then, the DC power flow with linear programming is used to calculate minimum load curtailments for all sampled states using (4)–(9). Finally, the obtained load curtailments using the DC power flow and linear programming for the sampled states are used to calculate the reliability indices. The rigorous procedure to evaluate composite power system reliability using the MCS can be found in [44,48]. The stopping criterion described in (18) is used to terminate the simulation. The tolerance level for β is used as ($\leqslant$0.025) [49]. The performed case studies for each of the adapted systems are described as follows.

4.1. Case I: reliability evaluation of the IEEE RTS

The total number of buses, generating units, and transmission lines of the IEEE RTS are 24, 32, and 38, respectively. The total generation capacity and peak load are 3405 MW and 2850 MW, respectively. The detailed data of the IEEE RTS are provided in [45]. Both the annualized and annual reliability indices are calculated.

To calculate the annualized indices using the proposed approach, 2000 unique samples are generated to train CNN. The training set contains 1424 failure states and 576 success states. The hyperparameters of the CNN and threshold to eliminate the prediction error of the trained network for this case are shown in the second row of Table 1. The hyperparameters are selected empirically. Since the input vector to the machine learning model includes available outputs at all the generating buses (10 generating buses), the capacity of all the transmission lines (38 transmission lines), and total load, the size of the input vector to the machine learning model for this case at any instance is 49. The output is the amount of load curtailment for each input sample.

It is worth mentioning here that several strategies such as data processing, feature engineering, appropriate model selection, parameter tuning, parameter optimization, etc. are integral parts for real applications of machine learning-based approaches, which are widely addressed in the existing related works. Although details on optimal parameter tuning, feature engineering, data cleaning, etc., are out of scope of this work, a training performances of several other approaches such as support vector machines, K-Nearest Neighbors, and Multi-Layer Perceptron are provided in Table 2 to validate effectiveness of the CNN. K-nearest Neighbor and Support Vector Machine models are taken as default from Scikit learn library. For Multi-layer perceptron the three hidden layers with 100 neurons in each layers and rectified linear unit as activation function is used. From Table 2, it can be seen that CNN shows better performance compared to the other machine learning models. Therefore, reliability indices are calculated only using the predictions obtained from the CNN. The variation in the training performances of the CNN for 15 different number of initial training samples for this case is shown in Fig. 3. From Fig. 3, it can be seen that the training performances are almost similar for all the initial training samples, which validates the robustness of the training procedure. The calculated annualized reliability indices for this case are provided in Table 3.

To calculate the annual reliability indices, a total number of 33,000 unique samples is generated among which 5620 are failure states and the remaining are success states. The RMSE, MAE, accuracy, precision, recall, and F_1 score of the trained network to calculate the annual reliability indices are 0.16243, 0.05387, 97.1496, 97.8425, 91.5456, and 94.5477, respectively. The hyperparameters of the CNN and threshold to eliminate the prediction error of the trained network to calculate annual indices of the IEEE RTS are shown in the third row of Table 1. Similar to the annualized indices, the hyperparameters to

Table 1
Hyperparameters of CNNs and threshold.

Systems	Hyper-parameters			
	CNN L, F, K	Dense L, N	A_H	A_O
IEEE RTS (Annualized)	2, 64, 3	3, 150	ReLU	Linear
IEEE RTS (Annual)	2, 64, 3	3, 100	ReLU	Linear
SPC	2, 64, 3	1, 100	ReLU	Linear
IEEE RTS-96	1, 64, 3	3, 300	ReLU	Linear

Note: L denotes number of layers, F denotes the filter size, K denotes kernel size, N denotes the number of neurons in a dense layer, A_H and A_O are the activation functions of hidden and output layers, respectively.

Table 2
Comparison of MLP, CNN, KNN, and Support Vector Machine (SVM) in terms of RMSE, MAE, precision, recall, and F_1 score for IEEE RTS and SPC.

Models	IEEE RTS					SPC				
	RMSE	MAE	P (%)	R (%)	F_1-Score	RMSE	MAE	P(%)	R (%)	F_1-Score
CNN	0.1038	0.022	100	97.10	98.53	0.047	0.0028	100	95.56	97.72
MLP	0.0855	0.0394	100	96.54	98.24	0.1830	0.0649	98.85	7.644	14.20
SVM	0.72	0.41	100	59.52	74.62	0.1806	0.0689	98.85	8.43	15.53
KNN	0.24	0.058	99.6	96.90	98.23	0.0917	0.0089	80.45	72.16	76.08

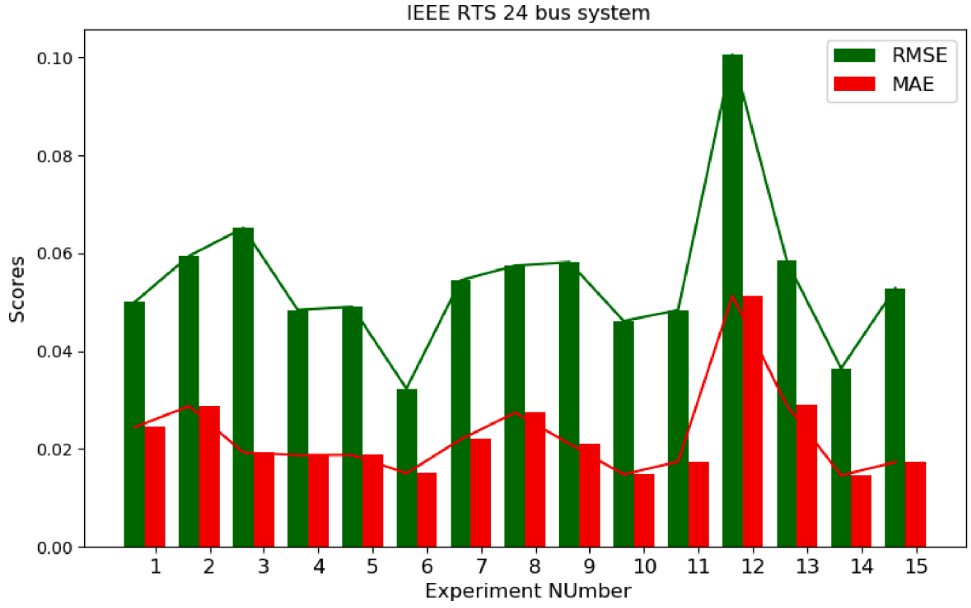

Fig. 3. Training performance for different number of initial training samples of the IEEE RTS.

Table 3
Annualized Reliability Indices for the IEEE RTS.

Reliability Indices	Methods		Difference (%)
	Proposed	MCS	
EDNS (MW/yr)	14.7111	14.7533	0.286
LOLP	0.08508	0.08505	0.035
LOLF (Occurrence/yr)	19.5969	19.4927	0.535

calculate annual indices are also selected empirically. Load clusters are typically used in calculating annual reliability indices of power systems [47,4]. Following the same convention, we have used load clusters to calculate annual reliability indices using both the proposed approach and MCS. CNN is trained for each cluster to calculate annual reliability indices using the proposed approach. For the low load levels, the number of success states is very high compared to failure states. Therefore, a large number of success states is discarded from the training samples (the ratio between the number of success states and failure states is kept $1:5$) to reduce the training time. The calculated annual indices of the IEEE RTS using the proposed method and MCS are shown in Table 4. The reduction in the number of OPF solutions and simulation time is discussed in Section 4.4.

Table 4
Annual Reliability Indices for the IEEE RTS.

Reliability Indices	Methods		Difference (%)
	Proposed	MCS	
EDNS (MW/yr)	0.12543	0.13134	4.50
LOLP	0.00118	0.00125	5.6
LOLF (Occurrence/yr)	0.41216	0.40086	2.82

4.2. *Case II: reliability evaluation of the SPC in Canada*

The SPC system consists of 29 generating units, 71 transmission lines, and 45 buses. The total generation capacity and annual peak load of the SPC are 25,300 MW and 18,025 MW, respectively. Among 45 buses, four buses are used to represent assistance from Manitoba Hydro System. One of the four buses is represented as a fictitious bus to import 300 MW power from the Manitoba Hydro System. The fictitious bus is connected with the remaining buses. The imported 300 MW power is represented using three independent generating units (each of 100 MW).

The detailed data of the SPC are also given in [50]. The DC power flow and linear programming are performed for $3,000$ unique training samples which contains 113 failure states and $2,887$ success states. Fourth row of Table 1 shows the hyperparameters and threshold. The hyperparameters for this case are also selected empirically. Since the input vector to the machine learning model includes the output at all the generation buses (8 generation buses), the capacity of all the transmission lines (71 transmission lines), and total load, the size of the input vector to the machine learning model for this case is 80. The output is the amount of the load curtailment. Table 2 shows the training performances of CNN compared to the other approaches for this case. Similar to *Case I*, K-nearest Neighbor and Support Vector Machine models are taken as default from Scikit learn library. For Multi-layer perceptron, three hidden layers with 150 neurons in each layer and rectified linear unit as activation function are used. Since CNN shows the comparable performance with other machine learning models and its performance is better for highly reliable practical power system model such as SPC, we have calculated the reliability indices only using the results obtained

from the CNN.

The calculated reliability indices for this case using the proposed method and MCS are provided in Table 5. The reduction in the number of OPF solutions and simulation time of the proposed method compared to the MCS is discussed in Section 4.4.

4.3. Case III: reliability evaluation of the IEEE RTS-96

The IEEE RTS-96 has 73 buses, 96 generating units, and 120 transmission lines. The total generation capacity and peak load of the IEEE RTS-96 are 10.21 GW and 8.55 GW, respectively. The detailed description of the IEEE RTS-96 is provided in [47]. The IEEE RTS-96 is very reliable, and therefore, loads and generators of the IEEE RTS-96 are increased by 40% to make it stressed.

To calculate the annualized indices for the IEEE RTS-96 using the proposed approach, a total number of 7000 unique samples are generated to train the CNN for this case. The number of failure and success states in the training data are 2451 and 4549, respectively. The size of the input vector for the IEEE RTS-96 is 151 (30 generation buses, 120 transmission lines, and one aggregate load). The RMSE, MAE, accuracy, precision, recall, and F_1 score of the trained network to calculate the annualized reliability indices are 0.40, 0.1479, 94.0366, 91.5254, 87.0967, and 89.2561, respectively. The hyperparameters of the CNN and threshold to eliminate the prediction error of the trained network to calculate annualized indices of the IEEE RTS-96 are shown in the fifth row of Table 1. The calculated annualized reliability indices for this case are provided in Table 6. The reduction in the number of OPF and simulation time for this case is also discussed in Section 4.4.

4.4. Results and discussion

The proposed method is implemented on the above-mentioned test systems. Annualized (for peak load) reliability indices are calculated for all the tested systems using both the proposed method and MCS. Also, to demonstrate the effectiveness of the proposed approach in calculating annual reliability indices, annual indices for the IEEE RTS are calculated as an example. In the first stage of the proposed approach, a CNN is trained to predict load curtailments. Then, predicted load curtailments are used to classify system states into failure and success states. Finally, load curtailments and classified system states are used to calculate the reliability indices.

Table 2 shows the performance of the proposed approach in terms of RMSE, MAE, precision (P), Recall (R), and F_1-score. From Table 2, we can see that the values of RMSE and MAE are very small, which indicate high accuracy in the predicted load curtailments. Also Table 2 shows that the values of P, R, and F-score are very high, which validate that the true prediction levels are almost perfect in the proposed approach. Therefore, it can be claimed that the proposed method can predict both the failure states and load curtailments in the failure states accurately.

Tables 3,5,6 show the calculated annualized reliability indices using both the proposed method and MCS for IEEE RTS and SPC, respectively. From Table 3, we can see that the difference in the calculated reliability indices using the proposed method and MCS vary from 0.035–0.535% for the IEEE RTS. Table 5 shows that the difference in the calculated reliability indices using the proposed method and MCS varies from 0.802–3.67% for the SPC. Table 6 shows that the difference in the calculated annualized reliability indices using the proposed method and MCS varies from 0.435–3.66% for the IEEE RTS-96. Table 4 shows that the calculated annual reliability indices using both the proposed method and MCS for IEEE RTS. The difference in the calculated annual reliability indices of the IEEE RTS using the proposed method and MCS vary from 2.82–5.6%. This indicates that the proposed method has high accuracy in calculating the reliability indices for the tested systems. Therefore, it can be concluded that the CNN can capture the complex pattern within input generations and loads and the output load curtailments precisely.

Table 7 shows the reduction in the number of OPF solutions and simulation time for the proposed method compared to the MCS.

From Table 7, it can be seen that the reduction in the number of samples that needs to perform the OPF to calculate annualized and annual indices of the IEEE RTS are 97.66% and 68.27%, respectively, less for the proposed method compared to the MCS. Table 7 also shows that the proposed method reduces 99.127% of samples that need solution of OPF compared to the MCS for the SPC. Moreover, from Table 7, we can see that the reduction in the number of samples for which the OPF needs to be solved for the proposed method is 91.81% compared to the MCS for the IEEE RTS-96. This happens because the proposed method uses the OPF only for a small number of training samples, and the trained network emulates the OPF using weights and biases for a large number of samples that require the calculation of the reliability indices. Also, Table 7 shows that the reduction in the number of samples that require OPF solutions is highest for the SPC system among the tested systems. This happens due to the fact that the SPC system is more reliable compared to the other tested systems, and it takes the highest number of samples to converge using the MCS. Moreover, Table 7 shows that the reduction in the simulation time for the SPC is significantly larger than the IEEE RTS and IEEE RTS-96. This happens because the same sequence is followed in the reduction of the number of samples that require to solve OPF.

The results show that the proposed approach not only calculates all the reliability indices with high accuracy but also is able to reduce the computational complexity and time significantly.

Also, the advantages of the proposed work over the state enumeration, improved Monte Carlo simulation, and previously proposed ML-based methods are demonstrated through a comparison analysis in

Table 5
Reliability Indices for the SPC-Canada.

Reliability Indices	Methods		Difference (%)
	Proposed	MCS	
EDNS (MW/yr)	0.0377	0.0374	0.802
LOLP	0.00105	0.00109	3.67
LOLF (Occurrence/yr)	0.88270	0.89097	0.92

Table 6
Annualized Reliability Indices for the IEEE RTS-96.

Reliability Indices	Methods		Difference (%)
	Proposed	MCS	
EDNS (MW/yr)	6.3615	6.6035	3.66
LOLP	0.02975	0.02988	0.435
LOLF (Occurrence/yr)	10.5656	10.3093	2.48

Table 7
Reduction in the number of DC power flow and simulation time for all the adapted systems.

Systems		Proposed method	MCS	Reduction
IEEE-RTS (Annualized)	OPF (No. of samples)	2,000	85,500	83,500
	Simulation time (s)	93.59	1652.28	1558.69
IEEE-RTS (Annual)	OPF (No. of samples)	33,000	104,000	71,000
	Simulation time (s)	778.203	1004.57	277.099
SPC	OPF (No. of samples)	3,000	344,000	341,000
	Simulation time (s)	130.91	4136.367	4005.457
IEEE RTS-96 (Annualized)	OPF (No. of samples)	7,000	85,500	78,500
	Simulation time (s)	508.844	1138.1861	629.342

Table 8
Comparison of state enumeration (SE), Monte Carlo simulation, improved Monte Carlo simulation, existing ML-based methods, and proposed methods.

Methods	No. of Samples	No. of power flow operation	Applicability	Computational cost
SE [21]	All the possible system states	For all the possible system states	To calculate LOLP, LOLF, and EDNS of small systems	Very high
MC simulation [44]	Significantly lower than SE. Calculated based on (18)	For all the sampled system states	To calculate LOLP, LOLF, and EDNS of small & medium systems	High
Improved MC simulation [7–13]	Significantly lower than SE. Calculated based on (18)	For all the sampled system states	To calculate LOLP, LOLF, and EDNS of small, medium, & large systems	High
Existing Ml-based [1–3,25–28]	Significantly lower than SE. Calculated based on (18)	Only for training samples (small No.)	To calculate LOLP & LOLF of all types (small, medium, large, & large integrated) systems	Less than ES, MC simulation, & improved MC simulation
Proposed	Significantly lower than SE. Calculated based on (18)	Only for training samples (small No.)	To calculate LOLP, LOLF, & EDNS of all types (small, medium, large, & very large integrated) systems	Less than ES, MC simulation, improved MC simulation, & other ML-based approaches

Table 8.

5. Conclusion and future work

This paper has proposed a CNN-based method to evaluate the reliability of composite power systems. The CNN was trained using samples that consist of generations, transmission line capacities, and total loads as input and total load curtailments as output. The training samples were generated using the MCS, linear programming technique, and DC power flow. After training the CNN, a new data set was fed as input to the trained CNN to calculate the reliability indices. This data set was generated based on the total loads and availability of generators and transmission lines. The predicted load curtailments were used to calculate the reliability indices without performing the OPF. Three case studies were carried out to analyze the effectiveness of the proposed method. In these case studies, the IEEE RTS, SPC, and IEEE RTS-96 were used to verify the effectiveness of the proposed method for different systems. The results showed that the OPF was performed for small number of samples in the proposed method, which reduces the computation complexity and simulation time significantly. The results also showed that the calculated reliability indices using the proposed method were close to those calculated using the OPF for each sampled state. Moreover, the results showed that the number of samples that require the solution of OPF for the proposed method for the tested systems are significantly lower compared to the Monte-Carlo simulation.

Incorporating several strategies such as data processing, hyperparameter optimization, feature engineering, etc. in the proposed approach are left as future scope of research. Also, analyzing the impacts of several composite load models on the performance of power system reliability methods can be a great scope of future research.

Source Code

The source code of this work is provided online (https://github.com/nbhusal/Composite-Reliability-Analysis-) for future research and development.

Declaration of Competing Interest

The authors declare that they have no known competing financial interests or personal relationships that could have appeared to influence the work reported in this paper.

Acknowledgement

This work was supported in part by the U.S. National Science Foundation (NSF) under Grant NSF 1847578.

References

[1] Pindoriya NM, Jirutitijaroen P, Srinivasan D, Singh C. Composite reliability evaluation using Monte Carlo simulation and least squares support vector classifier. IEEE Trans Power Syst 2011;26(4):2483–90.
[2] Urgun D, Singh C. A hybrid Monte Carlo simulation and multi label classification method for composite system reliability evaluation. IEEE Trans Power Syst 2019;34(2):908–17.
[3] Urgun D, Singh C, Vittal V. Importance sampling using multilabel radial basis classification for composite power system reliability evaluation. IEEE Syst J 2020;14(2):2791–800.
[4] da Silva AML, de Resende LC, da Fonseca Manso LA, Miranda V. Composite reliability assessment based on Monte Carlo simulation and artificial neural networks. IEEE Trans Power Syst 2007;22(3):1202–9.
[5] da Silva AML, de Resende LC, da Fonseca Manso LA, Miranda V. Artificial neural networks applied to reliability and well-being assessment of composite power systems. In: Proceedings of the 10th International Conference on Probablistic Methods Applied to Power systems, Rincon, Puerto Rico; 2008. p. 1–6.
[6] Luo X, Singh C, Patton AD. Power system reliability evaluation using self organizing map. In: IEEE Power Engineering Society Winter Meeting. Conference Proceedings (Cat. No.00CH37077), vol. 2, Singapore, Singapore; 2000. p. 1103–8.
[7] Green RC, Wang L, Singh C. State space pruning for power system reliability evaluation using genetic algorithms. In: IEEE PES General Meeting, Providence, RI, USA; 2010. p. 1–6.
[8] Zhao D, Singh C. Modified genetic algorithm in state space pruning for power system reliability evaluation and its parameter determination. In: North American Power Symposium, PArlington, TX, USA; 2010. p. 1–6.
[9] Singh C, Mitra J. Composite system reliability evaluation using state space pruning. IEEE Trans Power Syst 1997;12(1):471–9.
[10] Mitra J, Singh C. Pruning and simulation for determination of frequency and duration indices of composite power systems. IEEE Trans Power Syst 1999;14(3):899–905.
[11] Green RC, Wang Z, Wang L, Alam M, Singh C. Evaluation of loss of load probability for power systems using intelligent search based state space pruning. In: IEEE 11th International Conference on Probabilistic Methods Applied to Power systems, Singapore, Singapore; 2010. p. 319–24.
[12] Green RC, Wang L, Wang Z, Alam M, Singh C. Power system reliability assessment using intelligent state space pruning techniques: A comparative study. In: International Conference on Power System Technology, Hangzhou, China; 2010. p. 1–8.
[13] Green RC, Wang L, Alam M, Singh C. State space pruning for reliability evaluation using binary particle swarm optimization. In: IEEE/PES Power systems Conference and Exposition, Phoenix, AZ, USA; 2011. p. 1–7.
[14] Green RC, Wang L, Alam M, Singh C. Intelligent state space pruning using multi-objective PSO for reliability analysis of composite power systems: Observations, analyses, and impacts. In: IEEE Power and Energy Society General Meeting, Detroit, MI, USA; 2011. p. 1–8.
[15] Patra SB, Mitra J, Earla R. A new intelligent search method for composite system reliability analysis. In: IEEE/PES Transmission and Distribution Conference and Exhibition, Dallas, TX, USA; 2006. p. 803–7.
[16] Mitra J, Xu X. Composite system reliability analysis using particle swarm optimization. In: IEEE 11th International Conference on Probabilistic Methods Applied to Power systems, Singapore, Singapore; 2010. p. 548–52.
[17] Benidris M, Mitra J. Composite power system reliability assessment using maximum capacity flow and directed binary particle swarm optimization. In: North American Power Symposium, Manhattan, KS, USA; 2013. p. 1–6.
[18] Benidris M, Elsaiah S, Mitra J. Power system reliability evaluation using a state space classification technique and particle swarm optimisation search method. IET Gener Transmiss Distrib 2015;9(14):1865–73.
[19] Gonzlez-Fernndez RA, da Silva AML, Resende LC, Schilling MT. Composite systems reliability evaluation based on Monte Carlo simulation and cross-entropy methods. IEEE Trans Power Syst 2013;28(4):4598–606.
[20] Yong P, Zhang N, Kang C, Xia Q, Lu D. MPLP-Based fast power system reliability evaluation using transmission line status dictionary. IEEE Trans Power Syst 2019;34(2):1630–40.

[21] Lei Y, Hou K, Wang Y, Jia H, Zhang P, Mu Y, et al. A new reliability assessment approach for integrated energy systems: Using hierarchical decoupling optimization framework and impact-increment based state enumeration method. Appl Energy 2018;210(15):1237–50.
[22] Liu W, Cheng R, Xu Y, Liu Z. Fast reliability evaluation method for composite power system based on the improved eda and double cross linked list. IET Gener Transmiss Distrib 2017;11:3835–42.
[23] Liu W, Guo D, Xu Y, Cheng R, Wang Z, Li Y. Reliability assessment of power systems with photovoltaic power stations based on intelligent state space reduction and pseudo-sequential monte carlo simulation. Energies 2018;11(6):1–14.
[24] Khuntia SR, Rueda JL, van der Meijden MAMM. Mutual information based bayesian analysis of power system reliability. In: IEEE Eindhoven PowerTech, Eindhoven, Netherlands; 2015. p. 1–6.
[25] Urgun D, Singh C. Composite system reliability analysis using deep learning enhanced by transfer learning. In: International Conference on Probabilistic Methods Applied to Power Systems (PMAPS), Liege, Belgium; 2020. p. 1–6.
[26] Bera A, Chowdhury A, Mitra J, Almasabi S, Benidris M. Data-driven assessment of power system reliability in presence of renewable energy. In: International Conference on Probabilistic Methods Applied to Power Systems (PMAPS), Liege, Belgium; 2020. p. 1–6.
[27] Urgun D, Singh C. Lstm networks to evaluate composite power system reliability evaluation with injected wind power. In: IEEE Power Energy Society General Meeting (PESGM), Atlanta, GA, USA; 2019. p. 1–5.
[28] Mudgal S, Gupta PK, Yadav AK, Mahajan V. Artificial neural network for reliability evaluation of power system network with renewable energy. In: 21st National Power Systems Conference (NPSC), Gandhinagar, India; 2020. p. 1–6.
[29] Lei H, Singh C. Non-sequential Monte Carlo simulation for cyber-induced dependent failures in composite power system reliability evaluation. IEEE Trans Power Syst 2017;32(2):1064–72.
[30] Billinton R, Li W. A system state transition sampling method for composite system reliability evaluation. IEEE Trans Power Syst 1993;8(3):761–70.
[31] Mitra J, Singh C. Incorporating the DC load flow model in the decomposition-simulation method of multi-area reliability evaluation. IEEE Trans Power Syst 1996;11(3):1245–54.
[32] Krizhevsky A, Sutskever I, Hinton GE. Imagenet classification with deep convolutional neural networks. In: Advances in Neural Information Processing systems 25. Curran Associates Inc; 2012. p. 1097–105.
[33] Shi Z, Yao W, Zeng L, Wen J, Fang J, Ai X, et al. Convolutional neural network-based power system transient stability assessment and instability mode prediction. Appl Energy 2020;263:114586.
[34] Ju Y, Sun G, Chen Q, Zhang M, Zhu H, Rehman MU. A model combining convolutional neural network and lightgbm algorithm for ultra-short-term wind power forecasting. IEEE Access 2019;7:28309–18.
[35] Wang H, Yi H, Peng J, Wang G, Liu Y, Jiang H, et al. Deterministic and probabilistic forecasting of photovoltaic power based on deep convolutional neural network. Energy Convers Manage 2017;153:409–22.
[36] Wang S, Bi S, Zhang YJA. Locational detection of the false data injection attack in a smart grid: A multilabel classification approach. IEEE Internet Things J 2020;7(9):8218–27.
[37] Hou J, Xie C, Wang T, Yu Z, Lü Y, Dai H. Power system transient stability assessment based on voltage phasor and convolution neural network. In: 2018 IEEE International Conference on Energy Internet (ICEI). IEEE; 2018. p. 247–51.
[38] Gupta A, Gurrala G, Sastry P. An online power system stability monitoring system using convolutional neural networks. IEEE Trans Power Syst 2018;34(2):864–72.
[39] Samuel O, Javaid N, Khalid A, Khan WZ, Aalsalem MY, Afzal MK, et al. Towards real-time energy management of multi-microgrid using a deep convolution neural network and cooperative game approach. IEEE Access 2020;8:161377–95.
[40] Liang J, Jing T, Niu H, Wang J. Two-terminal fault location method of distribution network based on adaptive convolution neural network. IEEE Access 2020;8:54035–43.
[41] Kim J, Moon J, Hwang E, Kang P. Recurrent inception convolution neural network for multi short-term load forecasting. Energy Build 2019;194:328–41.
[42] Zhao Y, Tang Y, Li W, Yu J. Composite power system reliability evaluation based on enhanced sequential cross-entropy monte carlo simulation. IEEE Trans Power Syst 2019;34(5):3891–901.
[43] da Silva AML, Manso LADF, Mello JCDO, Billinton R. Pseudo-chronological simulation for composite reliability analysis with time varying loads. IEEE Trans Power Syst 2000;15(1):73–80.
[44] Bilinton R, Li W. Reliability Assessment of Electric Power systems Using Monte Carlo Methods. New York, NY, USA: Plenum; 1994.
[45] P.M. Subcommittee, IEEE reliability test system. IEEE Trans Power Sys 1979;PAS-98 (6):2047–54.
[46] Billinton R, Kumar S. Effect of higher-level independent generator outages in composite-system adequacy evaluation. IEE Proc C Gener Transmiss Distrib 1987;134(1):17–26.
[47] Grigg C, Wong P, Albrecht P, Allan R, Bhavaraju M, Billinton R, et al. The ieee reliability test system-1996. a report prepared by the reliability test system task force of the application of probability methods subcommittee. IEEE Trans Power Syst 1999;14(3):1010–20.
[48] Singh C, Jirutitijaroen P, Mitra J. Electric Power Grid Reliability Evaluation: Models and Methods. Wiley-IEEE Press; 2018.
[49] Mitra J, Singh C. Pruning and simulation for determination of frequency and duration indices of composite power systems. IEEE Trans Power Syst 1999;14(3):899–905.
[50] Billinton R, Kumar S. Effect of higher-level independent generator outages in composite-system adequacy evaluation. IEEE Proc C Gener Transmiss Distrib 1987;134(1):17–26.